

Can magma-injection and groundwater forces cause massive landslides on Hawaiian volcanoes?

Richard M. Iverson¹

U.S. Geological Survey, Cascades Volcano Observatory, 5400 MacArthur Blvd., Vancouver, WA 98661, USA

Received 7 December 1991; accepted 7 July 1994

Abstract

Landslides with volumes exceeding 1000 km³ have occurred on the flanks of Hawaiian volcanoes. Because the flanks typically slope seaward no more than 12°, the mechanics of slope failure are problematic. Limit-equilibrium analyses of wedge-shaped slices of the volcano flanks show that magma injection at prospective headscarps might trigger the landslides, but only under very restrictive conditions. If static magma weight is the sole source of magma pressure, hypothetical flank failures can have any size, but can occur only if slip-surface friction angles are less than about 16°. If slip surfaces have friction angles more typical of fragmented or intact rocks (30–40°), flank failures can occur only if mean magma pressures exceed static equilibrium pressures. Landslide length then scales with the excess magma pressure divided by the buoyant unit weight of the volcano flank. For typical excess magma pressures, buoyant unit weights and rock friction angles, the largest landslides that might be triggered in this manner have lengths of only several kilometers. This is at least an order of magnitude too small to explain the occurrence of giant Hawaiian landslides. The growing mass of active Hawaiian volcanoes can compress the edifice and substrate rocks and consequently produce groundwater head gradients that might destabilize larger sectors of the volcano flanks. However, calculations show that volcano growth at an estimated long-term vertical rate of 0.02 m/yr can generate significant head gradients only if an areally extensive, buried clay layer exists that has a great thickness (~200 m) or very low hydraulic diffusivity (~10⁻¹¹ m²/s). Additional calculations show that groundwater head gradients associated with topographically induced flow and sea-level change are less likely to be important. Thus a simple, quantitative explanation for failure of Hawaiian volcano flanks remains elusive, and more complex scenarios may merit investigation.

1. Introduction

Massive landslides play an important role in erosional degradation of many volcanoes. Widespread recognition of the significance of great landslides on subaerial stratovolcanoes resulted largely from the work of Glicken and his colleagues (Glicken, 1986, 1995; Voight et al., 1981, 1983; Crandell et al., 1984; Ui and Glicken, 1986; Brantley and Glicken, 1987;

Nakamura and Glicken, 1988; Siebert et al., 1989). Recent work has shown that giant landslides are also common on oceanic shield volcanoes, although much of the evidence is inconspicuous because it is submarine (e.g., Holcomb and Searle, 1991). Particularly noteworthy landslides have occurred on the Hawaiian Ridge, where they have removed volcano-flank sectors that exceed 1000 km³ in volume (Moore, 1964; Moore et al., 1989). Topographic and bathymetric data (Mark and Moore, 1987) indicate that, prior to failure, the sectors probably sloped less than 12° and almost certainly sloped less than 19°.

¹ I dedicate this paper to Harry Glicken, who enthusiastically introduced me to large volcanic landslides.

Failure of these gently sloping volcano flanks is problematic. A slope can fail gravitationally only if its average angle of inclination equals or exceeds the friction angle of the constituent soil or rock, unless additional forces are present. Friction angles of fragmented and intact rocks generally range from 25 to 50° (Jaeger and Cook, 1979, pp. 59–60; Lambe and Whitman, 1979, p. 146; Goodman, 1989, p. 83), and great rock-slides almost always occur on commensurately steep slopes (e.g., Voight, 1978). Gravitational failure of slopes inclined 12° or less typically occurs in subaerially weathered, low-friction clays or shales or in poorly compacted submarine sediments weakened by strong pore-fluid pressure gradients (e.g., Denlinger and Iverson, 1990; Baum and Fleming, 1991). Potential slip surfaces with such properties appear unlikely to exist within Hawaiian volcanoes that consist mostly of intercalated and fragmented lava flows, volcanogenic sediments and intrusions. Representative bulk friction angles of these materials have not been measured. However, observations of submarine talus deposits near Kilauea volcano, Hawaii, show that they typically slope 25 to 40° (Tribble, 1991), and representative friction angles thus may lie within this range. Unless giant Hawaiian landslides have failure surfaces with much lower friction angles, probably less than 12°, forces in addition to gravitation must trigger the landslides.

Magma injection can trigger giant volcanic landslides, a conclusion reached by Glicken and his colleagues in their assessment of the catastrophic Mount St. Helens rockslide-debris avalanche of May 18, 1980 (Voight et al., 1983; Glicken, 1986). Indeed, recent dike injection at Kilauea has been accompanied by seaward displacement of the volcano's south flank (Swanson et al., 1976; Delaney et al., 1990). Documented displacements are of the order of 10 m and affect an area of several hundred square kilometers. This might qualify the south flank of Kilauea as a giant landslide, although many previous investigators (e.g., Dieterich, 1988) have preferred to describe the displacement process as faulting. Regardless of terminology—landsliding or faulting—the findings of Swanson et al. (1976), Voight et al. (1983), Dieterich (1988), Moore et al. (1989) and Delaney et al. (1990) are consistent with the hypothesis that magma injection in Hawaiian volcanoes causes permanent seaward flank displacements that might culminate in flank collapse.

I evaluate this hypothesis by using a static, rigid-wedge, limit-equilibrium model to calculate the magma-injection and groundwater forces necessary to cause irreversible seaward displacements of Hawaiian volcano flanks. The calculations show that realistic magma-injection forces are unlikely to displace volcano flank sectors that exceed several kilometers in length, unless frictional resistance to sliding is anomalously low. Additional calculations show that groundwater forces that reduce friction sufficiently to destabilize larger flank sectors are unlikely to arise as a result of simple mechanical phenomena. However, the calculations quantify conditions under which large-scale failure *could* occur.

2. Rigid-wedge limit-equilibrium analysis

The limit-equilibrium analysis assumes that incipient seaward motion of a rigid, wedge-shaped slice of an oceanic volcano flank results from a static balance of driving and resisting forces along a potential slip surface. This is the most liberal mechanical assumption that can be used to assess failure potential; if all other factors are constant, driving forces that are too small to displace an ideal, rigid wedge are also too small to displace a deforming volcano flank.

The forces acting on a hypothetical, rigid wedge on the flank of an oceanic volcano, which slopes seaward at an angle ψ , are illustrated in Fig. 1. The wedge, with a size and shape that are unconstrained a priori, has an

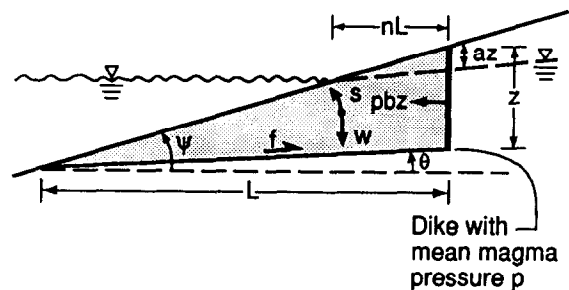


Fig. 1. Vertical cross section showing the geometry of a hypothetical landslide wedge of breadth b on the flank of an oceanic volcano. The wedge (shaded) is bounded upslope by a magma-filled dike. Bold arrows represent forces acting on the wedge: w is the buoyant weight force; s is the groundwater seepage force; f is the frictional resisting force; and pbz is the magma-pressure force, where p is the mean magma pressure.

arbitrary length L and breadth b . A fraction n ($0 \leq n \leq 1$) of the wedge length extends inland from sea level. A vertical dike of height z containing magma with mean pressure p bounds the wedge at its upslope margin and pushes seaward on the wedge. A fraction a ($0 \leq a \leq 1$) of the dike height extends above the sub-aerial water table. The base of the wedge is defined by a potential slip surface sloping at an angle θ , which may be either positive or negative, depending on whether the slip surface dips seaward or landward. A Coulomb friction force f along the potential slip surface resists seaward displacement of the wedge. I assume that the wedge length L and breadth b are much greater than the wedge thickness, and that frictional resistance on the sides of the wedge is negligible compared to f . Body forces acting on the wedge are those due to its buoyant weight w and groundwater seepage s . Only rigid-body translation of the wedge is of interest here, so the forces w and s can be resolved at the wedge centroid. Treatment of groundwater effects by considering buoyancy forces and arbitrary seepage forces is equivalent to a treatment that considers any conceivable distribution of pore pressures; the seepage-force approach holds the advantage of distinguishing between hydrostatic and hydrodynamic effects (cf. Iverson and Major, 1986; Iverson and Reid, 1992).

The wedge geometry and forces shown in Fig. 1 are similar to those considered by Dieterich (1988), whose approach, in turn, was similar to that used in sliding-wedge problems familiar to geotechnical engineers (e.g., Hoek and Bray, 1981, p. 150 ff.). My analysis differs from these previous analyses in two significant respects: (1) it allows magma pressures against the upslope margin of the wedge to deviate from static equilibrium pressures; (2) it accommodates an arbitrary seepage force (i.e., distribution of groundwater pressures), which is important for evaluating the possibility that groundwater helps trigger wedge displacement.

First, consider static equilibrium of the wedge in the absence of groundwater seepage ($s = 0$ in Fig. 1). Resolution of the weight w and magma-pressure force pbz into components normal and tangential to the potential slip surface at the base of the wedge shows that the mean effective normal stress σ and mean shear stress τ acting on the surface are given by:

$$\sigma = \frac{w \cos \theta - pbz \sin \theta}{(bL/\cos \theta)} \quad (1a)$$

$$\tau = \frac{w \sin \theta + pbz \cos \theta}{(bL/\cos \theta)} \quad (1b)$$

where $bL/\cos \theta$ is the area of the slip surface. A torque on the wedge may result from the magma-pressure force, pbz , which does not necessarily act through the wedge centroid. The torque must be resisted by a spatially variable effective normal stress along the base of the wedge. The rigid-wedge analysis neglects this spatial variability and considers only the mean effective normal stress σ , as defined by (1a).

Geometric analysis of Fig. 1 shows that the total volume of the wedge is $\frac{1}{2}Lzb$, and that the volume above the water table is $\frac{1}{2}Lzbna$. Thus the buoyant weight of the wedge is:

$$\begin{aligned} w &= (\frac{1}{2}Lzb - \frac{1}{2}Lzbna)(\gamma_r - \gamma_w) + \frac{1}{2}Lzbna\gamma_t \\ &= \frac{1}{2}Lzb(\gamma_r - \gamma_w + na\gamma_w) \\ &= \frac{1}{2}Lzb\gamma_t \end{aligned} \quad (2)$$

where γ_r is the unit weight of the solid rock, γ_w is the unit weight of groundwater that saturates the rock and γ_t is the mean buoyant unit weight of wedge (which accounts for the fact that part of the wedge may be above the water table). The weight of groundwater above the water table also can be included in γ_t , although this water produces no buoyancy force. Dieterich (1988) pointed out that rock densities may vary spatially around volcanic rift zones, with significant consequences for wedge stability. Here I regard γ_t as a mean value for the entire wedge; thus in the rigid-wedge analysis γ_t accounts implicitly for effects of spatially variable rock density. Table 1 shows that the value of γ_t likely lies in the range $10 \text{ kN/m}^3 \leq \gamma_t \leq 20 \text{ kN/m}^3$.

The mean magma pressure p includes both a static equilibrium component due to the mean magma unit weight γ_m and a mean excess-pressure component p_0 :

$$p = \frac{1}{z} \int_0^z \gamma_m z dz + p_0 = \frac{1}{2} \gamma_m z + p_0 \quad (3)$$

The presence of p_0 in Eq. (3) implies that either (1) the dike is capped, the magma is essentially static and the pressures within it differ from the static equilibrium

Table 1

Volcano-flank buoyant unit weights γ_i computed for various rock unit weights γ_r and percentages of the potential landslide volume that are unsubmerged na

na^b	γ_r^c	γ_i
0	20	10
0	23	13
0	26	16
0.36	20	14
0.36	23	17
0.36	26	20

Units for all values of γ_i and γ_r are kN/m^3 .

^a $na = 0$ represents complete submergence of the potential landslide; $na = 0.36$ represents subaerial exposure of more than half the landslide length ($n = 0.6$; $a = 0.6$).

^bThe limits $20 \text{ kN/m}^3 \leq \gamma_r \leq 26 \text{ kN/m}^3$ are based on rock bulk densities between 2.0 and 2.7 g/cm^3 , as discussed in detail by Dieterich (1988).

^c $\gamma_w = 10 \text{ kN/m}^3$ is assumed.

pressure by a mean amount p_0 ; or (2) magma is venting through a surface fissure, the downward pressure gradient in the flowing magma exceeds the static equilibrium gradient and the mean excess pressure is p_0 . In either case, p_0 can be no larger than the excess pressure that exists in the magma reservoir that feeds the dike.

Magnitudes of excess magma pressures are poorly constrained, even for an intensively studied, active volcano such as Kilauea. If laterally propagating dikes at Kilauea behave like pressurized cracks in linearly elastic media, magma pressures are likely to exceed lithostatic pressure by about 2 to 10 MPa at the center of the dike and by lesser amounts at the dike top and bottom (Rubin and Pollard, 1987). Pressures in dikes or conduits that erupt at the surface are more enigmatic. Some investigators have inferred that, at least within a few kilometers of the surface, magma-pressure gradients during eruptions are almost indistinguishable from lithostatic gradients (Delaney and Pollard, 1981; Wilson and Head, 1981) or are smaller than lithostatic gradients owing to high volume fractions of exsolved magmatic gas (Greenland et al., 1988). Other investigators have observed that Kilauea flank vents are fed from a well-defined shallow magma reservoir (Dvorak and Okamura, 1987), where magma pressures may exceed static pressures at flank vents by as much as 26 MPa prior to eruptions (Decker, 1987). Nearly all of this excess pressure presumably dissipates in transit as magma moves toward a flank vent during an eruption,

and it appears unlikely that mean excess magma pressures in erupting dikes exceed about 10 MPa. I consequently adopt $0 \leq p_0 \leq 10$ MPa as a reasonable range for p_0 .

I evaluate the frictional resisting force f by employing the well-known Coulomb rule:

$$\frac{f}{(bL/\cos \theta)} = \sigma \tan \phi \quad (4)$$

where ϕ is the angle of internal friction on the prospective slip surface. This form of the Coulomb rule represents only the frictional strength, $\sigma \tan \phi$. I assume bulk cohesive strength is negligible owing to the abundance of fractures in the volcanic rocks. Moreover, cohesive strength is generally negligible at the base of very thick landslides, where normal stress and attendant frictional strength far outweigh cohesion (cf. Denlinger and Iverson, 1990).

The Coulomb rule (4) can be used to determine a factor of safety, FS , defined as the ratio of frictional strength to driving stress along the potential slip surface:

$$FS = \frac{\sigma \tan \phi}{\tau} \quad (5)$$

Combination of (1a,b), (2), (3) and (5) and cancellation of redundant terms yields a factor-of-safety equation for the wedge:

$$FS = \frac{[L\gamma_i \cos \theta - (\gamma_m z + 2p_0) \sin \theta] \tan \phi}{L\gamma_i \sin \theta + (\gamma_m z + 2p_0) \cos \theta} \quad (6)$$

An explicit expression for the value of p_0 necessary to produce incipient motion or limiting equilibrium of the wedge results from setting $FS = 1$ in (6) and manipulating the resulting equation to obtain:

$$p_0 = \frac{L}{2} \gamma_i \frac{\cos \theta \tan \phi - \sin \theta}{\sin \theta \tan \phi + \cos \theta} - \frac{z}{2} \gamma_m \quad (7)$$

Eq. (7) represents a static balance between the forces due to w , p and f (with $s = 0$), shown in Fig. 1. The equation can be simplified by applying a trigonometric identity and the substitution $z = L(\tan \psi - \tan \theta)$ from Fig. 1 to reduce it to:

$$p_0 = \frac{L}{2} [\gamma_i \tan(\phi - \theta) - \gamma_m(\tan \psi - \tan \theta)] \quad (8)$$

This equation demonstrates two important points: (1) the length L of the wedge that can be pushed seaward by forceful magma injection is directly proportional to the excess magma pressure p_0 ; (2) if there is no excess magma pressure ($p_0 = 0$), the length of the wedge is indeterminate because the limit-equilibrium force balance (8) reduces to the scale-independent form:

$$\gamma_l \tan(\phi - \theta) = \gamma_m(\tan \psi - \tan \theta) \quad (9)$$

The scale-independence of (9), which is equivalent to eq. 12 of Dieterich (1988), results from the fact that all forces, including the seaward driving force due to static equilibrium magma pressure, are gravitational and scale with the dike height z (Fig. 1). Thus, (9) implies that very large landslides might be merely the consequence of very tall dikes. If any nonequilibrium magma pressure p_0 is present, however, scale-dependent failure governed by (8) will preempt the scale-independent failure governed by (9).

Normalization of (8), with (9) as a special case, allows graphs for all conceivable combinations of its variables to be represented on a single diagram. Employing a characteristic unit weight γ_l and characteristic length L , I normalize (8) by dividing all terms by $L\gamma_l$, which results in:

$$p_0^* = \frac{1}{2} [\tan(\phi - \theta) - \gamma^*(\tan \psi - \tan \theta)] \quad (10)$$

wherein $p_0^* = p_0 / (\gamma_l L)$ and $\gamma^* = \gamma_m / \gamma_l$. The characteristic unit weight probably lies in the range $10 \text{ kN/m}^3 \leq \gamma_l \leq 20 \text{ kN/m}^3$ (Table 1). The characteristic length, on the other hand, represents the landslide size, which is a key unknown. In Fig. 2 graphs of (10) are depicted for two values of p_0^* (0 and 0.5) and for three values of γ^* that correspond to the lower-bound, average and upper-bound edifice unit weights listed in Table 1. Graphs for combinations of p_0^* and γ^* not shown in Fig. 2 can be obtained easily by linear interpolation or extrapolation; for example, graphs for $p_0^* = 0.25$ would look exactly like those for $p_0^* = 0$ and $p_0^* = 0.5$, except that they would intersect the vertical axis where $\tan(\phi - \theta) = 0.5$.

The graphs of Fig. 2 illustrate three important points:

(1) The positive slope of all graphs shows that, for constant θ , as the volcano surface slope ($\tan \psi$) increases, the friction coefficient ($\tan \phi$) necessary to resist sliding increases in proportion. This occurs largely because the magmatic driving force increases with dike height and therefore with $\tan \psi$. It is consistent

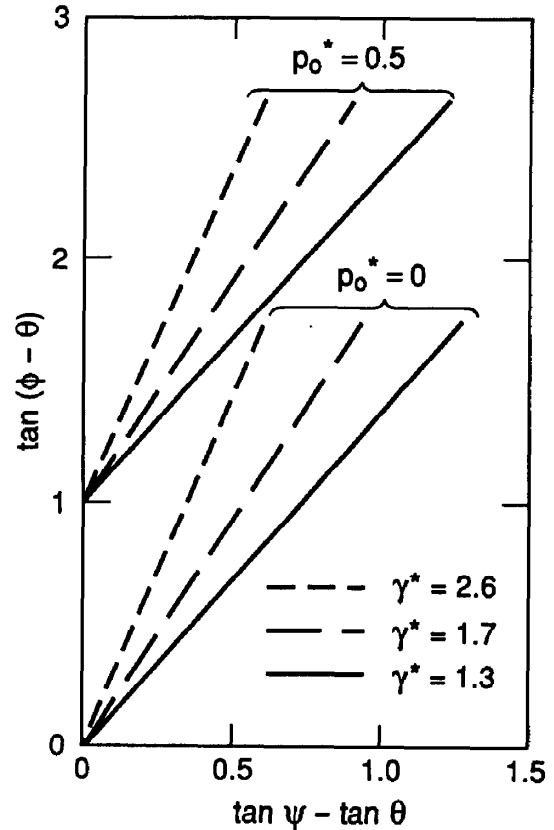


Fig. 2. Graphs of Eq. (10), showing limit-equilibrium relations between the friction angle ϕ , volcano-flank slope angle ψ and slip-surface angle θ , for various values of the normalized volcano unit weight γ^* and normalized excess magma pressure p_0^* .

with the inference of Moore and Clague (1992) that large-scale collapse of Hawaiian volcano flanks typically occurs near the end of shield construction, when the flanks are steepest.

(2) The constant of proportionality (i.e., the slope of the graphs) increases with decreases in the volcano edifice density. This occurs because the frictional resisting force depends directly on the weight of the overburden, whereas the magmatic driving force is independent of overburden weight.

(3) Limit-equilibrium conditions are very sensitive to the normalized excess magma pressure, p_0^* . For constant θ the coefficient of friction ($\tan \phi$) necessary to balance the driving and resisting forces in the case of $p_0^* = 0.5$ ranges from roughly 50% larger to infinitely larger than the coefficient of friction necessary in the case of no excess magma pressure ($p_0^* = 0$).

The advantage of complete generality is found in Fig. 2, but its normalized quantities can obscure the magnitudes of key variables. By depicting graphs of (8) and (9) with variables expressed in physical units, Fig. 3 helps remedy this shortcoming and provides a basis for comparing results with those of Dieterich (1988). The graphs of Fig. 3 apply for a particular magma unit weight, $\gamma_m = 26 \text{ kN/m}^3$, and volcano-flank slope, $\psi = 10^\circ$; these values are roughly representative of Hawaiian volcanoes (Zucca et al., 1982; Mark and Moore, 1987; Dieterich, 1988).

The curves for $p_0/L = 0$ in Fig. 3 show that the friction angle required to balance driving and resisting forces generally decreases with increases in slip-surface slope—a somewhat surprising result that is a consequence of the static magmatic driving force, which decreases as θ increases. The curves are similar to those in fig. 9 of Dieterich (1988), but differ in that they refer to values of the true friction angle, ϕ , rather than the apparent friction coefficient. (“True” means that effective stresses are used to calculate ϕ , with pore-water pressures explicitly taken into account; “apparent” means that pore pressures are included implicitly in the total stresses used to compute the friction coefficient.) All curves for $p_0/L = 0$ converge on $\phi = 10^\circ$ as the slip-surface slope approaches the volcano-surface slope, 10° . As the slip-surface slope decreases, the curves for different γ_t diverge markedly, illustrating

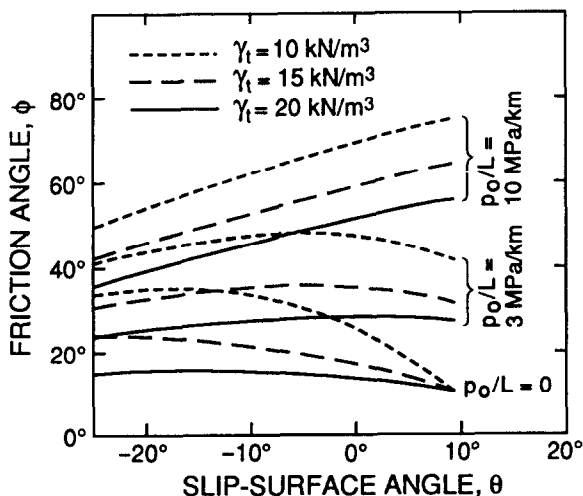


Fig. 3. Graphs of Eqs. (8) and (9), showing limit-equilibrium relations analogous to those of Fig. 2 but for a specific magma unit weight $\gamma_m = 26 \text{ kN/m}^3$ and volcano-flank slope $\psi = 10^\circ$.

the sensitivity to density noted by Dieterich (1988). For a slip surface oriented roughly horizontally, which Dieterich (1988) regarded as most plausible, the limit-equilibrium friction angles range from about 13 to 25° , depending on the edifice density. For a typical rock bulk density of 2500 kg/m^3 ($\gamma_t = 15 \text{ kN/m}^3$), limiting equilibrium requires $\phi \approx 16^\circ$, a value that is probably too low to be reasonable for volcanic rocks. Dieterich (1988) postulated that this low value is the result of a slip surface located at great depth in low-friction pelagic clay that underlies the volcano. An alternative hypothesis is that the slip surface might have a larger friction angle but that excess magma-pressure ($p_0 > 0$) or groundwater-seepage forces ($s > 0$) produce limiting equilibrium.

The curves for $p_0/L > 0$ in Fig. 3 show that both the magnitude and trend of the limit-equilibrium friction angles change markedly if excess magma pressure is present. With excess pressures of 3 MPa per km of slip-surface length, friction angles depend only weakly on the slip-surface slope, and limit-equilibrium conditions are satisfied for friction angles that range from about 22 to 47° , with values of 31 – 35° required for $\gamma_t = 15 \text{ kN/m}^3$. These ϕ values fall within a range that is reasonable for volcanic rocks. If excess magma pressures as large as 10 MPa/km are present, friction angles larger than 40° generally are required for limiting equilibrium. Thus excess magma pressures less than 10 MPa/km likely will suffice to trigger slope failure.

What is the maximum credible size of a landslide that might be triggered by injection of magma with excess pressure? Estimates based on Figs. 2 and 3 can vary widely, but the most useful estimates employ the most plausible combinations of friction angle and edifice density. For $\gamma_t = 15 \text{ kN/m}^3$ and ϕ in the range 30 – 40° , which I regard as most plausible, p_0/L will be about 3 MPa/km for typical volcano-flank slopes and magma densities (Fig. 3). If, as noted earlier, the maximum excess magma pressure is likely to be no more than 10 MPa , then the largest sector of the volcano flank likely to be displaced by magma injection has a length L of 3 – 4 km . Although this is only an order-of-magnitude estimate, it is noteworthy because it is at least an order of magnitude too small to explain the size of the giant Hawaiian landslides documented by Moore et al. (1989).

2.1. Static buoyancy effects

Buoyancy forces due to static groundwater and sea-water are included in all equations of the rigid-wedge flank-stability analysis described above. Thus Figs. 2 and 3 can be used to assess the static effects of increased volcano flank submergence, which may result from volcano subsidence and eustatic sea-level rise. Increased submergence decreases the value of γ_b , resulting in decreased flank stability. However, even complete submergence ($na=0$ in Fig. 1) results in buoyancy forces that appear insufficient to destabilize flank sectors with lengths greater than several kilometers, assuming that slip-surface friction angles are in the 30–40° range (Figs. 2 and 3). If friction angles are significantly smaller, however, or if friction is reduced by the effects of groundwater seepage (e.g., Iverson and Major, 1986), progressive submergence and increased buoyancy forces might trigger larger-scale flank failure. This possibility is noteworthy in the light of the inference of Moore and Clague (1992) that large-scale flank failures occur mostly near the end of Hawaiian volcanoes' shield-building phase, after kilometers of subsidence have occurred.

3. Groundwater-seepage effects

The effects of groundwater hydraulic gradients and attendant seepage modify the static, limit-equilibrium force balance described above. Predictable hydraulic gradients in an oceanic volcano might accompany at least three purely mechanical phenomena: (1) gravity-driven groundwater flow toward low elevations owing to rainfall recharge at higher, subaerial elevations; (2) relative sea-level change, which influences the boundary conditions for groundwater flow; (3) gravitational consolidation due to increasing overburden pressure caused by accumulating volcano mass. Hydraulic gradients might also arise more locally and less systematically as result of tectonic movements, such as faulting, or as a result of magma intrusion and thermal forcing. Neither of these effects is treated here.

The volume-averaged hydraulic head gradient, defined here as $-\nabla h$, and the volume over which it acts, V , determine the seepage force s of Fig. 1 (cf. Bear, 1972):

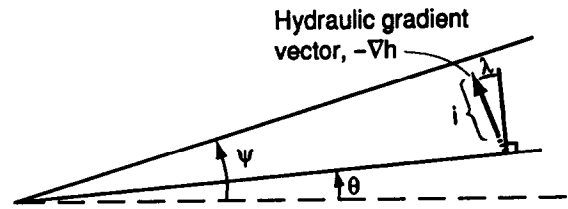


Fig. 4. Definition of the magnitude i and angular direction λ of the groundwater hydraulic gradient vector, $-\nabla h$. Note that λ is measured with reference to the hypothetical slip surface, not the slope surface (cf. Iverson and Major, 1986).

$$s = \gamma_w V (-\nabla h) \quad (11)$$

The seepage force can affect both the driving and resisting forces in a slope, depending on the direction of $-\nabla h$. Following the rationale detailed by Iverson and Major (1986), the seepage force can be resolved into orthogonal components that act in the direction of σ and τ , respectively:

$$s_\sigma = -\gamma_w V i \cos \lambda \quad (12a)$$

$$s_\tau = \gamma_w V i \sin \lambda \quad (12b)$$

in which i is the magnitude and λ is the angular direction of the hydraulic head gradient (Fig. 4). Significantly, the rigid-body limit-equilibrium analysis employs only the volume-averaged quantities i and λ ; details of the groundwater flow field that may result from hydraulic heterogeneity and anisotropy are irrelevant (cf. Iverson, 1990).

Inclusion of the seepage-force components (12a,b) in (1a,b) leads to modified expressions for the effective normal and shear stress:

$$\sigma = \frac{w \cos \theta - pbz \sin \theta - \gamma_w V i \cos \lambda}{(bL/\cos \theta)} \quad (13a)$$

$$\tau = \frac{w \sin \theta + pbz \cos \theta + \gamma_w V i \sin \lambda}{(bL/\cos \theta)} \quad (13b)$$

A factor-of-safety equation that accounts for groundwater-seepage results from employing (13a,b) rather than (1a,b) and repeating the steps that were used to obtain (6):

$$FS = \frac{\left[L\gamma_t \cos \theta - (\gamma_m z + 2p_0) \sin \theta - 2\gamma_w \frac{V}{bz} i \cos \lambda \right] \tan \phi}{L\gamma_t \sin \theta + (\gamma_m z + 2p_0) \cos \theta + 2\gamma_w \frac{V}{bz} i \sin \lambda} \quad (14)$$

Similarly, employing (14) and repeating the steps used to obtain (10) yields an equation for p_0^* that accounts for groundwater seepage:

$$p_0^* = \frac{1}{2} [\tan(\phi - \theta) - \gamma^* (\tan \psi - \tan \theta)] - \frac{\gamma_w i V}{\gamma_t V_{\text{tot}}} \zeta \quad (15)$$

in which ζ is a function defined by:

$$\zeta = \frac{\cos \lambda \tan \phi + \sin \lambda}{\sin \theta \tan \phi + \cos \theta} = \frac{\sin(\lambda + \phi)}{\cos(\phi - \theta)} \quad (16)$$

and $V_{\text{tot}} = \frac{1}{2} Lzb$ is the total volume of the potential landslide wedge, so that $V/V_{\text{tot}} = 1 - an$ (Fig. 1).

The last term in (15), $(\gamma_w/\gamma_t)i(V/V_{\text{tot}})\zeta$, referred to hereafter as the groundwater term, reflects the influence of groundwater seepage on the limit-equilibrium force balance. To estimate its value, estimates of γ_w/γ_t , i , V/V_{tot} and ζ are required. By far the best constrained of these parameters is γ_w/γ_t which plausibly ranges only between 0.5 and 1 (Table 1). The most poorly constrained parameter might appear to be ζ , which has a theoretical range of $-\infty$ to ∞ . However, Fig. 5 depicts graphs of ζ for all conceivable combinations of λ , θ and ϕ . The graphs show that for the most plausible values of these parameters ($20^\circ \leq \phi \leq 40^\circ$, $-10^\circ \leq \theta \leq 10^\circ$, $-10^\circ \leq \lambda \leq 190^\circ$) ζ varies only from 0 to about 2, and commonly $\zeta \approx 1$. (Values of $\lambda + \phi > 180^\circ$ are of no interest with respect to slope destabilization, because Fig. 5 shows that seepage in such instances acts to stabilize the slope.) The remainder of this section focuses on evaluating ζ , i , V/V_{tot} and the consequent value of the groundwater term for the most predictable mechanical phenomena that may produce seepage in Hawaiian volcanoes, as summarized in Table 2. The goal is not to determine precise values of the parameters but rather to estimate their possible influence on volcano-flank stability.

3.1. Gravity-driven groundwater flow

In many subaerial environments gravity-driven groundwater flow significantly affects slope stability (Iverson and Reid, 1992; Reid and Iverson, 1992). Furthermore, as a result of freshwater discharge to the

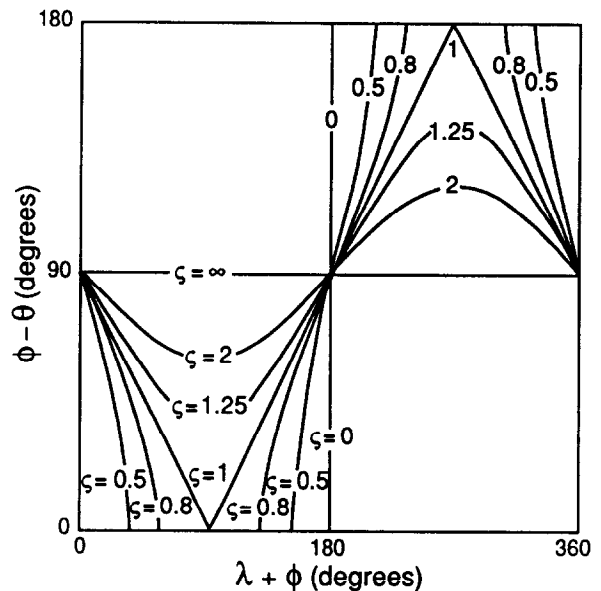


Fig. 5. Graph of the function ζ defined in Eq. (16). Only graphs for $\zeta \geq 0$ are shown. The graph for $\phi - \theta > 180^\circ$ is a mirror image of the graph for $0 \leq \phi - \theta \leq 180^\circ$.

sea floor, gravity-driven flow might affect submarine slope stability in near-shore areas. However, the magnitude of these effects depends on the gravitational hydraulic gradient, which can be no larger, on average, than the regional water-table slope. Evaluation of gravity-driven flow effects therefore requires assessment of water-table slopes.

A variety of field evidence indicates that water tables in the Hawaiian islands typically slope gently and that the water table typically rises no more than 10 m above sea level (Hunt et al., 1988). Low water-table elevations and slopes are also consistent with mathematical predictions, assuming that rainfall recharge of the water table averages no more than 2 m/yr and that permeabilities average at least 10^{-13} m^2 (0.1 darcy) (Forster and Smith, 1988a, b).

Inferences made from the locations of seeps and springs indicate that impoundment of water by low-permeability dikes produces locally steep gradients in Hawaiian water tables that are otherwise nearly flat (Stearns and MacDonald, 1946). Such impoundment probably explains Kilauea borehole logs that document water-saturated rocks 614 m above sea level at distances only about 20 km inland (Zablocki et al., 1974). Still, a water table at this elevation represents an overall

Table 2

Computation of maximum plausible value of the groundwater (GW) term in equation 15 for various groundwater-flow scenarios

Scenario	Parameter values used to compute GW term				Maximum GW term ^b	Comments
	i	$\frac{V}{V_{\text{tot}}}$	λ (%)	ζ^a		
No groundwater flow ($-\nabla h = 0$)	0	–	–	–	0	
Gravity-driven flow	≤ 0.05	0.2	90	0.9–1.2	~ 0.01	Steady state
Flow due to sea-level change ^c	~ 0	–	–	–	~ 0	For uniform $D \geq 10^{-4}$ m ² /s and failure depth 250 m
Flow due to sea-level change ^c	~ 0.1	≤ 0.5	0	0.3–0.8	~ 0.03	For uniform $D = 10^{-8}$ m ² /s and failure depth 250 m
Flow due to sea-level change ^c	~ 0.1	≤ 0.5	0	0.3–0.8	~ 0.03	For 10-m-thick layer with $D = 10^{-11}$ m ² /s and failure depth 250 m
Flow due to volcano growth and substrate consolidation ^d	~ 0	–	–	–	~ 0	For substrate layer 20 m thick with $D \geq 10^{-8}$ m ² /s
Flow due to volcano growth and substrate consolidation ^d	~ 0.1	≤ 1	0	0.3–0.8	~ 0.06	For substrate layer 20 m thick with $D = 10^{-11}$ m ² /s

^aAssumes plausible ranges of ϕ and θ to be $20^\circ \leq \phi \leq 40^\circ$ and $-10^\circ \leq \theta \leq 10^\circ$.

^bEmploys the maximum ζ from the previous column and $\gamma_w/\gamma_t = 0.8$.

^cAssumes a 20 m sea-level decline in 10,000 yr.

^dAssumes a vertical volcano-growth rate of 0.02 m/yr for at least 300,000 yr.

borehole-to-sea water-table slope of less than 2° . Thus, even with dike impoundment of water, it appears unlikely that the average water-table slope between a prospective landslide headscarp and the sea exceeds 3° . I consequently regard $i = \tan 3^\circ \approx 0.05$ as a maximum value of the mean hydraulic gradient associated with gravity-driven groundwater flow in Hawaiian volcanoes.

Using the estimate $i = 0.05$ along with $\gamma_w/\gamma_t = 1$, $\zeta = 1$ (based on a hydraulic gradient direction that, on average, parallels the slope) and the generous estimate that 20% of the wedge volume experiences such a gradient ($V = V_{\text{tot}}/5$), I estimate the maximum magnitude of the groundwater term in (15) to be about 0.01 (Table 2). In Fig. 2 it is shown that the other terms on the right-hand side of (15) typically have much greater magnitudes, except in the trivial case in which the prospective landslide wedge is very thin ($\psi \approx \theta$) and the volcano flank slopes at nearly the angle of repose ($\psi \approx \phi$). Thus, I infer that gravity-driven groundwater flow plays an insignificant role in triggering giant landslides on Hawaiian volcanoes.

3.2. Groundwater flow due to relative sea-level change

Relative sea-level change influences the submarine and shoreline boundary conditions that control ground-

water flow in Hawaiian volcanoes. Although increases in relative sea levels due to volcano subsidence and eustatic sea-level rise enhance the buoyancy forces on a prospective landslide wedge, they generate inward-directed hydraulic gradients ($180^\circ \leq \lambda + \phi \leq 360^\circ$ in Figs. 4 and 5) that help stabilize the wedge. Declining relative sea levels, on the other hand, produce outward-directed hydraulic gradients ($0^\circ \leq \lambda + \phi \leq 180^\circ$ in Figs. 4 and 5), that help destabilize the wedge. Consequently, I focus here on the possible *destabilizing* effects of relative sea-level decline.

Relative sea-level decline can, on average, steepen the subaerial water-table slope in an oceanic volcano only by an amount equal to the magnitude of the sea-level decline divided by the volcano radius. Relative sea-level declines on Hawaiian volcanoes have almost certainly been less than 100 m and have probably been less than 20 m, because volcano subsidence rates nearly matched eustatic sea-level decline rates during Pleistocene glaciations (Moore and Clague, 1992). Hawaiian volcano radii generally exceed 10 km, so the resulting mean water-table slope increases of perhaps $20 \text{ m} \div 10 \text{ km} = 0.002$ would contribute negligibly to seepage forces, as shown in the previous section.

Sea-level decline also reduces the hydraulic head on the sea floor, which might produce significant upward

hydraulic gradients normal to the sea floor. If sufficiently large, such gradients can destabilize even deposits that slope just a few degrees (Denlinger and Iverson, 1990).

Several factors, however, severely limit production of hydraulic gradients by relative sea-level decline. First, significant gradients can arise only if the relative sea level declines faster than the rate of hydraulic head diffusion in sea-floor sediments. Otherwise, reduction of hydraulic heads at depth will keep pace with sea-level decline and no strong gradients will develop. Sea-level declines occur in conjunction with widespread glaciations that probably require at least 10,000 yr (Andrews, 1987), so hydraulic head diffusion must occur more slowly than this for significant hydraulic gradients to develop. Moreover, poroelastic calculations by Roeloffs (1988) show that a significant fraction of even an instantaneous head decline at the sea floor would be balanced by a contemporaneous head decline at all depths in the sea-floor sediments. This occurs if the sediment grains and pore water are much less compressible than is the sea-floor sediment as a whole.

Lower-bound estimates of hydraulic head diffusion rates can be based on a simple, uncoupled, one-dimensional diffusion model (cf. Bredehoeft and Hanshaw, 1968; Roeloffs, 1988):

$$\frac{\partial h}{\partial t} = D \frac{\partial^2 h}{\partial y^2} \quad (17)$$

in which D is the hydraulic diffusivity, y is the depth into the sediment and t is time. Diffusivity is directly proportional to sediment permeability and inversely proportional to sediment compressibility. Plausible values of diffusivity range from about 10^{-4} to 10^2 m²/s in crustal rocks and from about 10^{-11} to 10^{-5} m²/s in clays (cf. Li, 1985; Lambe and Whitman, 1979). Employing the auxiliary conditions $h = h_0$ everywhere at $t = 0$ and $h = 0$ at $y = 0$ for $t > 0$ with (17) yields the well-known error-function solution (Carslaw and Jaeger, 1959, p. 59):

$$\frac{h}{h_0} = \operatorname{erf} \frac{1}{2} \left(\frac{y^2}{Dt} \right)^{1/2} \quad (18)$$

This equation describes the minimum speed and maximum attenuation of a head change as it diffuses to any depth y (cf. Roeloffs, 1988). It illustrates a fundamen-

tal property of all diffusion solutions: t scales with the quantity y^2/D , where y represents the characteristic diffusion path length. Consequently, I present graphs of various diffusion solutions that depict the normalized head or head gradient as a function of the dimensionless time Dt/y^2 .

In Fig. 6 a graph of (18) is depicted. It shows that for diffusivities that may be typical of lithified lava flows, $D \sim 1$ m²/s (Versey and Singh, 1982), hydraulic head changes diffuse to depths y of at least a kilometer in a few years, negating the hypothesis that relative sea-level declines produce significant hydraulic gradients. The graph also shows that if a clay layer with an exceedingly low diffusivity of $D = 10^{-11}$ m²/s and thickness of 10 m were buried at a depth of 250 m in the volcanic edifice, a hydraulic gradient $i \approx 0.1$, averaged through the 250-m thickness, could result from a 10,000-yr relative sea-level decline of 20 m because negligible head diffusion would occur in the clay. A 250-m thickness of more typical clay, with $D = 10^{-8}$ m²/s, would be required to produce the same effect, and with $D = 10^{-4}$ m²/s diffusion occurs so rapidly that no significant head gradient could be produced (Table 2).

Estimates of the maximum plausible groundwater effects due to relative sea-level decline assume that a low-diffusivity clay layer *does* exist at a depth no greater than 250 m and that slow head diffusion *does* occur. The induced hydraulic gradient might affect, at most, half the landslide wedge ($V \approx V_{\text{tot}}/2$). The gradient would be directed almost vertically, so that $\zeta \approx 1$

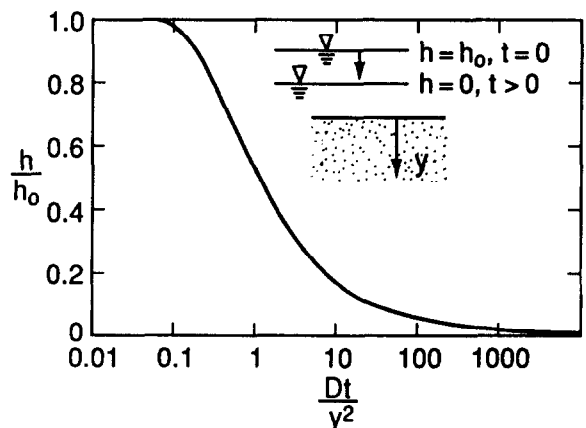


Fig. 6. Graph of Eq. (18), illustrating diffusion of a step change in hydraulic head at the surface of a half space as a function of the dimensionless time Dt/y^2 , where y is the depth below the surface (modified from Bredehoeft and Hanshaw, 1968).

would be reasonable (Fig. 5). Consequently, the groundwater term in (15) would be no larger than about 0.03 (Table 2). In most circumstances a term of this size would have little effect on the limit-equilibrium force balance. Thus the effects of sea-level decline on volcano-flank stability are likely to be small.

3.3. Groundwater flow due to edifice consolidation

Hawaiian volcanic edifices undoubtedly consolidate (i.e., compress) as well as subside under the great weight of accumulating lava flows and intrusions. Consolidation might be accompanied by significant hydraulic head gradients—depending on the relative rates of overburden loading and induced groundwater flow. Consolidation is, in fact, the same process as hydraulic head diffusion; only the driving force and domain geometry distinguish consolidation from the diffusion that accompanies sea-level change. If the driving force is simply gravitation acting on a rock mass of fixed size, one-dimensional consolidation obeys the homogeneous diffusion Eq. (17). However, if the gravitational driving force changes with time, as it does in a growing volcano, an inhomogeneous term $\gamma_1(dl/dt)$ enters the diffusion equation (Gibson, 1958):

$$\frac{\partial h}{\partial t} = D \frac{\partial^2 h}{\partial y^2} - \gamma_1 \frac{dl}{dt} \quad (19)$$

in which l is the mean volcano thickness at any time and dl/dt is the volcano accretion rate.

The ages and heights of young Hawaiian volcanoes help constrain volcano accretion rates. The oldest known rocks of Mauna Kea, for example, date to roughly 400,000 yr B.P. (Clague and Dalrymple, 1987), and the volcano rises roughly 9000 m above its submarine base. Thus an estimate of the maximum plausible long-term vertical accretion rate is $9000/400,000 \approx 0.02$ m/yr. The vertical accretion rate undoubtedly varies in space and time, but a long-term maximum of 0.02 m/yr nonetheless appears adequate for order-of-magnitude calculations.

Gibson (1958) derived an analytical solution of (19) for a steadily accreting, areally infinite domain underlain by an impermeable base. In this case dl/dt is a constant, and the accretion rate is simply l/t , assuming $l=0$ at $t=0$. Bredehoeft and Hanshaw (1968) employed Gibson's solution to analyze consolidation and groundwater flow in accreting sedimentary basins,

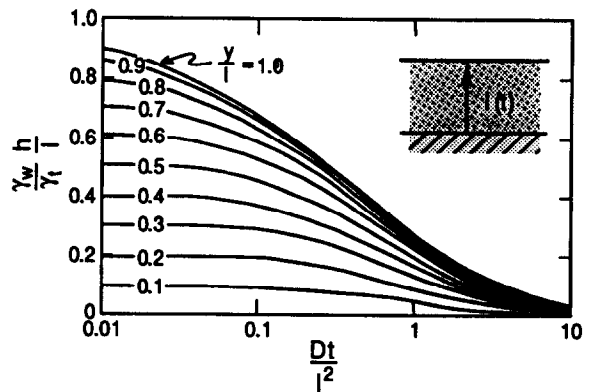


Fig. 7. Graph of the solution of Eq. (19), showing the hydraulic head distribution in a consolidating half space that grows vertically at a steady rate l/t . Normalized heads are plotted as a function of the dimensionless time Dt/l^2 , where l is the half-space thickness; y is the depth below the half-space surface (modified from Bredehoeft and Hanshaw, 1968).

and I use his solution in the same manner to analyze accreting volcanoes. However, consolidation of a volcano is not one-dimensional, and groundwater can escape by pathways other than vertical. As a consequence, hydraulic gradients estimated using solutions of (19) represent *maximum* gradients that might exist in a consolidating volcano.

In Fig. 7 graphs of Gibson's (1958) solution of (19) are depicted and normalized heads at different depths within the consolidating material. Note that the length scale in this case is l , which grows with time. The upward head gradient, which is proportional to the spacing between the curves, depends strongly on Dt/l^2 . For $Dt/l^2 > 10$, the hydraulic gradient approaches zero and has little consequence for stability. For $Dt/l^2 < 0.01$, the hydraulic gradient approaches the lithostatic gradient, which would reduce the effective stress and frictional strength in the edifice to nearly zero, with very large consequences for flank stability. The smallest conceivable values of Dt/l^2 occur during the last stages of volcano growth, when l is largest. Employing a maximum l (9000 m) and a maximum accretion rate of $l/t = 0.02$ m/yr, I find that $D < 6 \times 10^{-5}$ m²/s is required to give $Dt/l^2 < 10$. Such a diffusivity is implausibly low for rocks, but is typical of clays. Consequently, hydraulic gradients caused by consolidation of a volcano will have little influence on edifice stability, unless areally extensive clay layers are present at depth.

The most readily identifiable clay layer associated with growing oceanic shield volcanoes is the underlying layer of pelagic sediment. The growing weight of the volcano undoubtedly consolidates this layer and perhaps produces significant hydraulic gradients. This situation differs from that in which the volcano itself consolidates, because only the load, and not the consolidating layer thickness, grows with time. Schiffman (1958) solved the problem of a finite-thickness clay layer consolidating under a load that increases linearly with time. In this case dl/dt in (19) is again constant, and the accretion rate is simply l/t if $l=0$ at $t=0$ is assumed.

To facilitate interpretation of the solution of Schiffman (1958), I first recast his eq. 46 in terms of the volcano-accretion loading rate $\gamma_t(l/t)$. I then differentiate the resulting equation with respect to the dimensionless time Dt/δ^2 , which yields an equation with dependent and independent variables comparable to those of Fig. 7:

$$\frac{\gamma_w \bar{h}}{\gamma_t l} = \frac{8}{\pi^2} \sum_{n=1,3,5} \frac{1}{n^2} \exp\left(-\frac{n^2 \pi^2 Dt}{4 \delta^2}\right) \quad (20)$$

in which \bar{h} is the average excess head in the clay layer and the length scale is δ , defined as half the clay-layer thickness. Since in general $\delta \ll l$, \bar{h}/l provides an estimate of the average hydraulic head gradient i affecting the volcanic edifice.

In Fig. 8 a graph of (20) is depicted, which shows that the head gradient \bar{h}/l declines with time, in part

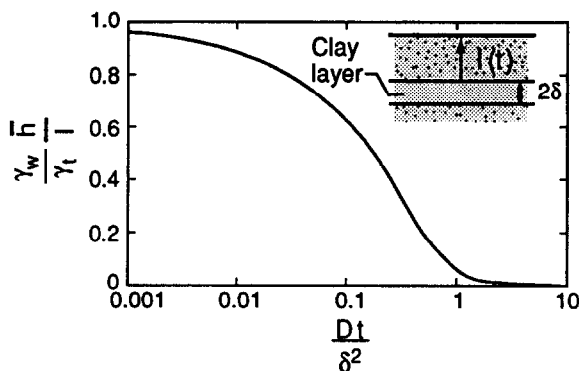


Fig. 8. Graph of Eq. (20), showing the mean hydraulic head in a consolidating clay layer overlain by a high-permeability material with unit weight γ_t and a thickness that increases steadily at a rate l/t . Normalized heads are plotted as a function of the dimensionless time Dt/δ^2 , where δ is half the clay-layer thickness.

because l increases with time. Very large gradients occur for dimensionless times less than 0.01, but these gradients have limited significance because the corresponding volcano thickness l is very small. Comparison of Figs. 7 and 8 shows that, for dimensionless times larger than 0.01, the average head gradient \bar{h}/l appears to decline more sharply in the case of a consolidating, finite-thickness clay layer than in the case of a consolidating volcano. This apparent effect is deceptive, however, because the diffusivity D of the clay layer may be ten or more orders of magnitude smaller than that of the volcanic rocks. For example, for a clay layer with $\delta = 10$ m and $D = 10^{-11}$ m²/s, the time scale δ^2/D for consolidation and groundwater head diffusion is 10^{13} s or about 300,000 yr. This is many orders of magnitude longer than the time scale for consolidation of the volcano itself if $D \approx 1$ m²/s in the edifice. Thus, after 300,000 yr of volcano growth, a mean hydraulic gradient i ($=\bar{h}/l$) as large as 0.1 might persist as a consequence of a consolidating basal clay layer but not as a consequence of a consolidating volcanic edifice (Figs. 7 and 8). Groundwater discharge from the clay layer would be mostly upward ($\zeta \approx 1$) and would affect nearly the entire volcano. Thus the groundwater term in (15) could be larger than for any of the alternative scenarios, and could be significant (Table 2). However, development of strong hydraulic gradients as a result of consolidation requires the presence of a clay layer with very low hydraulic diffusivity. For example, if D is as large as 10^{-8} m²/s, induced hydraulic gradients are negligible because the time scale δ^2/D for consolidation of a layer with $\delta = 10$ m reduces to only 300 yr, which is considerably less than the time required for significant volcano growth.

4. Concluding discussion

Employing a rigid-wedge limit-equilibrium analysis, I have evaluated the balance of forces that affect stability of Hawaiian volcano flanks. The analysis assumes that flank displacement is driven by gravitational, magma-pressure and groundwater-seepage forces and is resisted by Coulomb friction along the wedge base.

If both magma and groundwater have static equilibrium pressure distributions ($p_0 = 0$ and $s = 0$), the limit-equilibrium force balance is scale independent. The

size of potential volcano-flank landslides is then constrained only by flank geometry. However, slope failure in this instance is problematic because slip at the base of the wedge requires an anomalously low basal friction angle ($\phi < \sim 16^\circ$). Moreover, the presence of any non-gravitational force ($s \neq 0, p_0 \neq 0$) preempts scale-independent failure and causes the size of potential landslides to scale with excess magma-pressure and groundwater-seepage forces.

Excess pressure ($p_0 > 0$) in a magma body that bounds the wedge upslope enhances the potential for slope failure. However, if the slip-surface friction angle is similar to that of typical fractured and intact rocks ($\phi = 30\text{--}40^\circ$), excess magma pressure must be roughly 3 MPa per km of slip-surface length to cause failure. Previous work constrains excess magma pressures in feeder conduits at Kilauea volcano, Hawaii, to be no more than about 10 MPa. Thus, landslides no longer than several kilometers appear likely to be triggered by excess magma pressure alone. Such lengths are roughly an order of magnitude less than those of giant Hawaiian landslides.

Groundwater-seepage forces might lower the frictional resistance to sliding and combine with magma pressures to trigger giant landslides. Significant groundwater head gradients can arise only under rather specific circumstances, however. Simple calculations show that neither topographically induced groundwater flow nor the effects of relative sea-level change are likely to be important. Consolidation of a buried clay layer under the growing weight of the volcanic edifice might produce more significant seepage forces, but only if the clay layer is either very thick (hundreds of meters) or has a very low hydraulic diffusivity ($\sim 10^{-11} \text{ m}^2/\text{s}$).

Lack of a simple yet general mechanical explanation for failure of Hawaiian volcano flanks points to the possible role of more complex phenomena. Perhaps progressive weakening of slip-surface materials occurs, resulting in anomalously low friction angles. Strong earthquake shaking might momentarily modify the equilibrium force balance and initiate catastrophic sliding. Thermal stressing and groundwater convection induced by intrusions might be important. Alternatively, a sequence of small events that eventually lead to catastrophic failure might occur: kilometer-scale, local flank failure might load adjacent slopes and lead to progressively more widespread failure. Better

knowledge of volcano-flank properties is needed to assess such possibilities.

Acknowledgements

I thank Roger Denlinger, James Ewart, Homa Lee, Larry Mastin, Jim Moore, Mark Reid, Evelyn Roeloffs, Andy Simon and Barry Voight for discussion and criticism that helped improve this paper.

References

- Andrews, J.T., 1987. The late Wisconsin glaciation and deglaciation of the Laurentide ice sheet. In: W.F. Ruddiman and H.E. Wright (Editors), *North America and Adjacent Oceans during the Last Deglaciation*. (The Geology of North America, Vol. K-3). Geol. Soc. Am., Boulder, CO, pp. 13–38.
- Baum, R.L. and Fleming, R.W., 1991. Use of longitudinal strain in identifying driving and resisting elements in landslides. *Geol. Soc. Am. Bull.*, 103: 1121–1132.
- Bear, J., 1972. *The Dynamics of Fluids in Porous Media*. Dover, New York, NY, 764 pp.
- Brantley, S. and Glicken, H., 1987. Volcanic debris avalanches. *Earthquakes and Volcanoes*, 18: 195–206.
- Brederhoeft, J.D. and Hanshaw, B.B., 1968. On the maintenance of anomalous fluid pressures: I. thick sedimentary sequences. *Geol. Soc. Am. Bull.*, 79: 1097–1106.
- Carslaw, H.S. and Jaeger, J.C., 1959. *Conduction of Heat in Solids*. Oxford Univ. Press, Oxford, 510 pp.
- Clague, D.A. and Dalrymple, G.B., 1987. The Hawaiian–Emporer volcanic chain: Part I. Geologic evolution. In: R.W. Decker, T.L. Wright and P.H. Stauffer (Editors), *Volcanism in Hawaii*. U.S. Geol. Surv., Prof. Pap., 1350: 5–55.
- Crandell, D.R., Miller, C.D., Glicken, H.X., Christiansen, R.L. and Newhall, C.G., 1984. Catastrophic debris avalanche from ancestral Mount Shasta, California. *Geology*, 12: 143–146.
- Decker, R.W., 1987. Dynamics of Hawaiian volcanoes: an overview. In R.W. Decker, T.L. Wright and P.H. Stauffer (Editors), *Volcanism in Hawaii*. U.S. Geol. Surv., Prof. Pap., 1350: 997–1018.
- Delaney, P.T. and Pollard, D.D., 1981. Deformation of host rocks and flow of magma during growth of minette dikes and breccia-bearing intrusions near Ship Rock, New Mexico. *U.S. Geol. Surv., Prof. Pap.* 1202, 61 pp.
- Delaney, P.T., Fiske, R.S., Miklius, A., Okamura, A.T. and Kato, M.K., 1990. Deep magma body beneath the summit and rift zones of Kilauea volcano, Hawaii. *Science*, 247: 1311–1316.
- Denlinger, R.P. and Iverson, R.M., 1990. Limiting equilibrium and liquefaction potential of infinite submarine slopes. *Mar. Geotechnol.*, 9: 299–312.
- Dieterich, J.H., 1988. Growth and persistence of Hawaiian volcanic rift zones. *J. Geophys. Res.*, 93: 4258–4270.
- Dvorak, J.J. and Okamura, A.T., 1987. A hydraulic model to explain variations in summit tilt rate at Kilauea and Mauna Loa volca-

- noes. In R.W. Decker, T.L. Wright and P.H. Stauffer (Editors), *Volcanism in Hawaii*. U.S. Geol. Surv., Prof. Pap., 1350: 1281–296.
- Forster, C. and Smith, L., 1988a. Groundwater flow systems in mountainous terrain: 1. Numerical modeling technique. *Water Resour. Res.*, 24: 999–1010.
- Forster, C. and Smith, L., 1988b. Groundwater flow systems in mountainous terrain: 2. Controlling factors. *Water Resour. Res.*, 24: 1011–1023.
- Gibson, R.E., 1958. The progress of consolidation in a clay layer increasing in thickness with time. *Geotechnique*, 8: 171–182.
- Glicken, H., 1986. Rockslide-debris avalanche of May 18, 1980, Mount St. Helens Volcano, Washington. Ph.D. Thesis, Univ. California, Santa Barbara, CA, 303 pp. (unpubl.).
- Glicken, H., 1995. Rockslide-debris avalanche of May 18, 1980, Mount St. Helens Volcano, Washington. U.S. Geol. Surv., Prof. Pap. (in press).
- Goodman, R.E., 1989. *Introduction to Rock Mechanics*. Wiley, New York, NY, 562 pp.
- Greenland, L.P., Okamura, A.T. and Stokes, J.B., 1988. Constraints on the mechanics of the eruption. In: E.W. Wolfe (Editor), *The Puu Oo Eruption of Kilauea Volcano, Hawaii: Episodes 1 through 20, January 3, 1983 through June 8, 1984*. U.S. Geol. Surv., Prof. Pap., 1463: 155–164.
- Hoek, E. and Bray, J.W., 1981. *Rock Slope Engineering*. Inst. Min. Metall., London, 3rd rev. ed., 358 pp.
- Holcomb, R.T. and Searle, R.C., 1991. Large landslides from oceanic volcanoes. *Mar. Geotechnol.*, 10: 19–32.
- Hunt, C.D., Ewart, C.J. and Voss, C.I., 1988. Region 27, Hawaiian Islands. In: W. Back, J.S. Roseshein and P.R. Seaber (Editors), *Hydrogeology. (The Geology of North America, Vol. O-2)*. Geol. Soc. Am., Boulder, CO, pp. 255–262.
- Iverson, R.M., 1990. Groundwater flow fields in infinite slopes. *Geotechnique*, 40: 139–143.
- Iverson, R.M. and Major, J.J., 1986. Groundwater seepage vectors and the potential for hillslope failure and debris-flow mobilization. *Water Resour. Res.*, 22: 1543–1548.
- Iverson, R.M. and Reid, M.E., 1992. Gravity-driven groundwater flow and slope failure potential: 1. Elastic effective-stress model. *Water Resour. Res.*, 28: 925–938.
- Jaeger, J.C. and Cook, N.G.W., 1979. *Fundamentals of Rock Mechanics*. Chapman and Hall, London, 3rd ed., 593 pp.
- Lambe, T.W. and Whitman, R.V., 1979. *Soil Mechanics*, SI Version. Wiley, New York, NY, 553 pp.
- Li, V.C., 1985. Estimation of in-situ diffusivity of rock masses. *Pure Appl. Geophys.*, 22: 545–559.
- Mark, R.G. and Moore, J.G., 1987. Slopes of the Hawaiian Ridge. In: R.W. Decker, T.L. Wright and P.H. Stauffer (Editors), *Volcanism in Hawaii*. U.S. Geol. Surv., Prof. Pap., 1350: 255–262.
- Moore, J.G., 1964. Giant submarine landslides on the Hawaiian Ridge. U.S. Geol. Surv., Prof. Pap., 501-D: D95–D98.
- Moore, J.G. and Clague, D.A., 1992. Volcano growth and evolution of the island of Hawaii. *Geol. Soc. Am. Bull.*, 104: 1471–1484.
- Moore, J.G., Clague, D.A., Holcomb, R.T., Lipman, P.W., Normark, W.R. and Torresan, M.E., 1989. Prodigious submarine landslides on the Hawaiian Ridge. *J. Geophys. Res.*, 94: 17,465–17,484.
- Nakamura, Y. and Glicken, H., 1988. Blast and debris avalanche deposits of the 1888 eruption, Bandai Volcano. *J. Geogr. (Jpn.)*: 67–74.
- Reid, M.E. and Iverson, R.M., 1992. Gravity-driven groundwater flow and slope failure potential: 2. Effects of slope morphology, material properties, and hydraulic heterogeneity. *Water Resour. Res.*, 28: 939–950.
- Roeloffs, E.A., 1988. Fault stability changes induced beneath a reservoir with cyclic variations in water level. *J. Geophys. Res.*, 93: 2107–2124.
- Rubin, A.M. and Pollard, D.D., 1987. Origin of blade-like dikes in volcanic rift zones. In: R.W. Decker, T.L. Wright and P.H. Stauffer (Editors), *Volcanism in Hawaii*. U.S. Geol. Surv., Prof. Pap., 1350: 1449–1470.
- Schiffman, R.L., 1958. Consolidation of soil under time-dependent loading and varying permeability. *Proc. 37th Annu. Meet. Highway Research Board*, Washington, DC, pp. 584–617.
- Siebert, L., Glicken, H. and Kienle, J., 1989. Debris avalanches and lateral blasts at Mount Augustine Volcano, Alaska. *Natl. Geogr. Res.*, 5: 232–249.
- Stearns, H.T. and MacDonald, G.A., 1946. *Geology and groundwater resources of the Island of Hawaii*. Hawaii Div. Hydrogr. Bull. 9, 363 pp.
- Swanson, D.A., Duffield, W.A. and Fiske, R.S., 1976. Displacement of the south flank of Kilauea volcano: the result of forceful intrusion of magma into rift zones. U.S. Geol. Surv., Prof. Pap. 963, 30 pp.
- Tribble, G.W., 1991. Underwater observations of active lava flows from Kilauea Volcano, Hawaii. *Geology*, 19: 633–636.
- Ui, T. and Glicken, H., 1986. Internal structure variations in a debris avalanche deposit from ancestral Mount Shasta, California. *Bull. Volcanol.*, 48: 189–194.
- Versey, H.R. and Singh, B.K., 1982. Groundwater in the Deccan basalts of the Betwa Basin, India. *J. Hydrol.*, 58: 279–306.
- Voight, B. (Editor), 1978. *Rockslides and Avalanches, 1 Natural Phenomena*. Elsevier, New York, NY, 833 pp.
- Voight, B., Glicken, H., Janda, R.J. and Douglas, P.M., 1981. Catastrophic rockslide-avalanche of May 18. In: P.W. Lipman and D.R. Mullineaux (Editors), *The 1980 Eruptions of Mount St. Helens, Washington*. U.S. Geol. Surv., Prof. Pap., 1250: 347–377.
- Voight, B., Janda, R.J., Glicken, H. and Douglas, P.M., 1983. Nature and mechanics of the Mount St. Helens rockslide-avalanche of 18 May 1980. *Geotechnique*, 33: 243–273.
- Wilson, L. and Head III, J.W., 1981. Ascent and eruption of basaltic magma on the Earth and Moon. *J. Geophys. Res.*, 86: 2971–3001.
- Zablocki, C.J., Tilling, R.I., Peterson, D.W. and Christiansen, R.L., 1974. A deep research drill hole at the summit of an active volcano, Kilauea, Hawaii. *Geophys. Res. Lett.*, 1: 323–326.
- Zucca, J.J., Hill, D.P. and Kovach, R.L., 1982. Crustal structure of Mauna Loa Volcano, Hawaii, from seismic refraction and gravity data. *Bull. Seismol. Soc. Am.*, 72: 1535–1550.